

Atomic Carbon in APM 08279+5255 at $z=3.91$ ¹

J. Wagg,^{2,3} D.J. Wilner,² R. Neri,⁴ D. Downes,⁴ and T. Wiklind,⁵

²*Harvard-Smithsonian Center for Astrophysics, Cambridge, MA, 02138*

`hwagg@cfa.harvard.edu`

³*Instituto Nacional de Astrofísica, Óptica y Electrónica (INAOE), Aptdo. Postal 51 y 216, Puebla, Mexico*

⁴*Institut de Radio Astronomie Millimétrique, St. Martin d'Hères, F-38406, France*

⁵*ESA Space Telescope Division, STScI, 3700 San Martin Drive, Baltimore, MD 21218, USA*

ABSTRACT

We present a detection of [CI] $^3P_1-^3P_0$ emission in the lensed quasar APM 08279+5255 at $z=3.91$ using the IRAM Plateau de Bure interferometer. The [CI] line velocity and width are similar to the values of previously detected high-J CO and HCN lines in this source, suggesting that the emission from all of these species arises from the same region. The apparent luminosity of the [CI] line is $L'_{\text{CI}} = (3.1 \pm 0.4) \times 10^{10} \text{ K km s}^{-1} \text{ pc}^2$, which implies a neutral carbon mass, $M_{\text{CI}} = (4.4 \pm 0.6)m^{-1} \times 10^7 M_{\odot}$, where m is the lensing magnification factor. The [CI] line luminosity is consistent with the large molecular gas mass inferred from the nuclear CO line luminosity ($\sim 10^{11}m^{-1} M_{\odot}$). We also present an upper limit on the H₂O $1_{10}-1_{01}$ line luminosity in APM 08279+5255 of, $L'_{\text{H}_2\text{O}} < 1.8 \times 10^{10} \text{ K km s}^{-1} \text{ pc}^2$ ($3\text{-}\sigma$).

Subject headings: – galaxies: active – galaxies: high-redshift – quasars: emission lines – quasars: individual (APM 08279+5255) – galaxies: ISM

¹Based on observations carried out with the IRAM Plateau de Bure Interferometer. IRAM is supported by INSU/CNRS (France), MPG (Germany) and IGN (Spain).

1. Introduction

The ultraluminous quasar APM 08279+5255 at $z=3.91$ (Irwin et al. 1998) is strongly gravitationally lensed (Ledoux et al. 1998; Ibata et al. 1999; Egami et al. 2000) and appears to be one of the most luminous objects in the Universe, with an apparent infrared luminosity of $\sim 10^{15} L_{\odot}$ (Lewis et al. 1998). Observations over a wide range of wavelengths (e.g., Downes et al. 1999; Ellison et al. 1999; Gallagher et al. 2002; Soifer et al. 2004; Wagg et al. 2005) have shown that APM08279+5255 contains an active nucleus and likely a starburst component.

The combination of extreme intrinsic luminosity and amplification by strong gravitational lensing has allowed APM 08279+5255 to be detected in many rotational lines of CO (J=4-3 and J=9-8 Downes et al. 1999, hereafter D99; J=1-0 and J=2-1 Papadopoulos et al. 2001; Lewis et al. 2002), including the unique detection in the high excitation J=11-10 line (A. Weiss et al., in preparation). From high angular resolution observations, D99 suggest that the high-J CO emission arises in a warm, dense circumnuclear disk of sub-kiloparsec size. The detection of both HCN J=5-4 and HCO⁺ J=5-4 line emission support the idea that the molecular gas is dense (Wagg et al. 2005; Garcia-Burillo et al. 2006)

Given the wealth of molecular lines detected in APM 08279+5255, observations of additional diagnostic lines can provide further constraints on the physical conditions in this high-redshift object. One important tracer of the dense neutral gas within a galaxy’s interstellar medium is atomic carbon, in particular the [CI] $^3P_1-^3P_0$ line with rest frequency 492.161 GHz (Gérin & Phillips 1998, 2000). This line has not been observed widely in local galaxies due to poor atmospheric transmission near this frequency; however, this line is redshifted into better atmospheric windows for objects at redshifts, $z \gtrsim 1$. The [CI] $^3P_1-^3P_0$ line provides a complimentary probe of the physical conditions of dense, neutral gas, and the [CI]/CO ratio may also provide information on the role of X-rays in the molecular excitation (Maloney et al. 1996). In addition, Papadopoulos et al. (2004a, b) argue that this line can provide a measure of the total molecular hydrogen (H₂) gas mass, independent of CO line emission.

To date, [CI] emission has been detected in four objects at $z > 2$, most of which are thought to be gravitationally lensed. The $^3P_1-^3P_0$ line was first detected in H1413+117 at $z=2.6$ (the “Cloverleaf”; Barvainis et al. 1997), and more recently the higher excitation $^3P_2-^3P_1$ line was also detected in this object (Weiss et al. 2003). Other high-redshift objects with [CI] $^3P_1-^3P_0$ line detections include IRAS F10214 at $z=2.3$ (and an upper-limit on the [CI] $^3P_2-^3P_1$ line intensity is reported by Papadopoulos 2005), SMM J14011+0252 at $z=2.6$ (Weiss et al. 2005), and PSS 2322+1944 at $z=4.1$ (Pety et al. 2005).

Another important species that acts as a major coolant of dense gas is water. In general,

H₂O lines at local velocities are not accessible from the ground, but they have been observed from space and are ubiquitous in dense molecular cloud cores in the Galaxy (Ashby et al. 2000; Snell et al. 2000). At high-redshift, a tentative detection of the H₂O 2₁₁–2₀₂ line, with rest frequency 752.033 GHz, was reported in IRAS F10214 at $z=2.3$ (Encrenaz et al. 1993; Casoli et al. 1994). At more modest redshifts, the fundamental transition of ortho-water, H₂O 1₁₀–1₀₁ has been detected in absorption towards B0218+357 at $z=0.685$ (Combes & Wiklind 1997). For APM 08279+5255, the lower excitation H₂O 1₁₀–1₀₁ line with rest frequency 556.936 GHz is redshifted into the 3 millimeter atmospheric window.

Here we report a detection of [CI] ³P₁–³P₀ line emission in APM 08279+5255 at $z=3.91$, and an upper-limit on H₂O 1₁₀–1₀₁ line emission, obtained with the IRAM Plateau de Bure Interferometer (PdBI). Throughout this paper we adopt a Λ -dominated cosmology: $H_0 = 70 \text{ km s}^{-1} \text{ Mpc}^{-1}$, $\Omega_\Lambda = 0.7$, and $\Omega_m = 0.3$ (Spergel et al. 2006).

2. Observations

We used the IRAM PdBI to search for the [CI] ³P₁–³P₀ and H₂O 1₁₀–1₀₁ lines in APM 08279+5255, redshifted to the 3-millimeter band, on six dates in 1999 and 2001. All of the observations were made in compact configurations of the four or five available antennas. The receivers were tuned to 100.216 GHz for the [CI] line, and 113.406 GHz for the H₂O line. Spectral correlators covered a velocity range of $\sim 1500 \text{ km s}^{-1}$ for [CI], and $\sim 1300 \text{ km s}^{-1}$ for H₂O. The phase center was offset by 1.25'' from the CO peak position in D99. Baseline lengths ranged from 17 to 81 meters, and the synthesized beam sizes were 7''2 × 6''0 (position angle 89°) for the [CI] image, and 5''9 × 4''4 (position angle 82°) for the H₂O image. The nearby quasar 0749+540 was used for complex gain calibration. The flux scale was set using standard sources including MWC349, CRL618, 3c345.3 and 0923+392, and should be accurate to better than 20%. The on-source integration time for the [CI] and H₂O images were equivalent to 7.3 hours and 3.1 hours, respectively, with the full six antenna array. The resulting [CI] image has an rms noise of 0.36 mJy beam⁻¹ in a 150 km s⁻¹ channel, and the H₂O image has a higher rms noise of 0.96 mJy beam⁻¹ in a 130 km s⁻¹ channel, reflecting lower atmospheric transmission near the edge of the 3-millimeter window.

3. Results

Figure 1 shows images of the [CI] line and continuum emission over the full velocity range observed. The line emission is clearly detected in several velocity bins and appears

spatially unresolved. The position of peak emission is consistent with that found previously for the dust continuum, CO lines, and HCN line. Figure 2 shows the spectra of the [CI] and H₂O lines at this position. There is no evidence for significant H₂O line emission. For the [CI] spectrum, we estimate the continuum level at 100.2 GHz using the “line-free” channels to be $S_{100\text{GHz}} = 1.18 \pm 0.18$ mJy. For the H₂O spectrum, we estimate the continuum level at 113.4 GHz using all of the channels to be $S_{113\text{GHz}} = 2.43 \pm 0.48$ mJy. These values are consistent with the 93.9 GHz continuum flux of 1.20 ± 0.30 mJy measured by D99 and a thermal spectrum. A Gaussian fit to the continuum subtracted [CI] $^3\text{P}_1-^3\text{P}_0$ spectrum yields a peak of 2.20 ± 0.51 mJy, central velocity $v_0 = 117 \pm 28$ km s⁻¹ ($z=3.9130 \pm 0.0005$), and $\Delta V_{\text{FWHM}} = 386 \pm 67$ km s⁻¹. The integrated intensity of the [CI] $^3\text{P}_1-^3\text{P}_0$ line is 0.93 ± 0.13 Jy km s⁻¹, which implies a line luminosity $L'_{\text{CI}} = (3.1 \pm 0.4) \times 10^{10}$ K km s⁻¹ pc², following Solomon et al. (1992). Table 1 lists the fitted and derived [CI] $^3\text{P}_1-^3\text{P}_0$ line parameters.

We place an upper limit on the H₂O $1_{10}-1_{01}$ line emission from the noise around the mean in the spectrum, assuming $\Delta V_{\text{FWHM}} = 450$ km s⁻¹ like the CO, HCN, and [CI] lines. The $3\text{-}\sigma$ upper limit to the integrated intensity is $3 \cdot (\Delta V_{\text{FWHM}}/\Delta V_{\text{chan}})^{1/2} \cdot \sigma_{\text{chan}} = 0.70$ Jy km s⁻¹, which implies an upper limit to the H₂O line luminosity $L'_{\text{H}_2\text{O}} < 1.8 \times 10^{10}$ K km s⁻¹ pc².

4. Discussion

4.1. Emission Region and [CI]/CO Luminosity Ratio

The fitted [CI] line center and width are compatible with previous observations of the HCN J=5-4 and HCO+ J=5-4 lines (Wagg et al. 2005; Garcia-Burillo et al. 2006), though offset by ~ 120 km s⁻¹ from the mean redshift determined from the high-J CO lines (D99; Weiss et al. 2006, in preparation). While the line center difference between the [CI] and CO is formally significant at the $\sim 4\sigma$ level, the true significance is likely lower, since the line profiles from this complex source are almost certainly not described accurately by a single Gaussian. Given this uncertainty, the modest signal-to-noise ratios, and the lack of any resolved velocity structure in the observed line profiles, we simplify our analysis by assuming the [CI] emission region is cospatial with the CO line emission region, such that the conditions derived for a model with a single physical component apply to both species. We stress that even if all of the observed lines do arise from a single physical component, the fitted Gaussian centers and widths of lines with different excitation properties will not necessarily match each other perfectly, given the complexity of the underlying source structure and optical depth effects. Data of higher quality and from more transitions will be required to relax the single

component assumption and to justify more sophisticated modeling.

The gas in the single component region is warm and dense, and is likely to be a circumnuclear disk of sub-kiloparsec size. The CO emission clearly has been magnified by gravitational lensing, and models suggest a magnification factor in the range 3 to 20 (D99, Lewis et al. 2002), or even higher in the models by Egami et al. (2000). The exact magnification factor depends critically on the intrinsic size of the emitting region. If the [CI], CO, and HCN emission are truly co-spatial, however, then the magnification factors are the same, and line luminosity ratios will not suffer any biases due to differential lensing effects.

The luminosity ratio between the [CI] and CO lines is a potential diagnostic of the gas excitation and carbon chemistry. To compare the luminosities of [CI] and CO in APM 08279+5255, we use the nuclear component of the CO J=1-0 emission (Lewis et al. 2002), which gives $L'_{[CI]}/L'_{CO(1-0)} = 0.23 \pm 0.06$. This value falls within the range 0.2 ± 0.2 found for local galaxies (Gérin & Phillips 2000), and also the range $\sim 0.15 - 0.32$ for the other four high-redshift objects that have been detected in both [CI] and CO emission. This ratio does not appear to have any strong dependence on environment, either in the local galaxy sample, or at high-redshifts. Given the significant uncertainties in the [CI]/CO luminosity ratio for any individual object, it is not possible to place strong constraints on the contribution of X-ray irradiation to the molecular gas excitation.

We can estimate the [CI/CO] abundance ratio from the observations, adopting the physical conditions derived from multi-transition CO observations (Wagg et al. 2005; A. Weiss et al. in preparation) and a simple radiative transfer model. Using the *RADEX*² LVG code (Schöier et al. 2005), we find that an abundance ratio, [CI/CO] ~ 0.6 , reproduces the observed [CI] $^3P_1 - ^3P_0$ to CO J=1-0 line luminosity ratio. This ratio is similar to that found in the nearby starburst galaxy M82 ([CI/CO] ~ 0.5 ; Schilke et al. 1993, White et al. 1994).

4.2. Neutral Carbon Mass

The luminosity of the [CI] $^3P_1 - ^3P_0$ line can be used to derive the neutral carbon mass (Weiss et al. 2005), as

$$M_{[CI]} = 5.706 \times 10^{-4} \frac{Q(T_{ex})}{3} e^{23.6/T_{ex}} L'_{[CI]} [M_{\odot}], \quad (1)$$

where $Q(T_{ex}) \sim 1 + 3e^{-T_1/T_{ex}} + 5e^{-T_2/T_{ex}}$ ($T_1 = 23.6$ K and $T_2 = 62.5$ K are the energies of the 3P_1 and 3P_2 levels above the ground state) is the partition function. The only high-redshift

²<http://www.strw.leidenuniv.nl/~moldata/radex.html>

object for which both the [CI] $^3P_1-^3P_0$ and [CI] $^3P_2-^3P_1$ lines have been measured is the “Cloverleaf” quasar, where $T_{ex} = 30$ K (Weiss et al. 2003, 2005). Without a measurement of the higher [CI] $^3P_2-^3P_1$ line in APM 08279+5255, the value of T_{ex} is uncertain. However, Weiss et al. (2005) show that for $T_{ex} > 20$ K and LTE, the estimated neutral carbon mass is insensitive to the assumed excitation temperature. Adopting a nominal value of $T_{ex} = 80$ K for the [CI] $^3P_1-^3P_0$ line in APM 08279+5255 (from the derived molecular gas and dust temperatures), the neutral carbon mass within the nuclear region of APM 08279+5255 is $M_{\text{CI}} = (4.4 \pm 0.6)m^{-1} \times 10^7 M_{\odot}$, where m is the lensing magnification factor. If T_{ex} were 20 K, then the estimated [CI] mass would be $\sim 30\%$ lower.

4.3. Molecular Gas Mass

The luminosity in the CO J=1-0 line is the traditional tracer of molecular gas (= H₂) mass in the Galaxy and in a variety of extragalactic environments. For nearby ultraluminous infrared galaxies (ULIRGs; Sanders & Mirabel 1996; Sanders et al. 1988), which are believed to be analogues to the currently detectable luminous high-redshift galaxies, the empirical scaling factor between CO J=1-0 luminosity and H₂ gas mass is $\sim 1 M_{\odot} (\text{K km s}^{-1} \text{ pc}^2)^{-1}$ (Downes & Solomon 1998). If we apply this factor to the nuclear CO J=1-0 line emission in APM 08279+5255 (Papadopoulos et al. 2001; Lewis et al. 2002), then the molecular gas mass implied is $\sim 1.5m^{-1} \times 10^{11} M_{\odot}$.

Following Papadopoulos et al. (2004a), the small scatter in the observed [CI]/CO luminosity ratio suggests that [CI] $^3P_1-^3P_0$ emission may provide an independent estimate of molecular gas mass. Papadopoulos et al. (2004a) relate the integrated [CI] line intensity, $S_{[\text{CI}]}$, to molecular (= H₂) gas mass, as

$$M_{\text{H}_2-[\text{CI}]} = 1375.8 \frac{D_l^2}{1+z} \left(\frac{X_{[\text{CI}]}}{10^{-5}} \right)^{-1} \left(\frac{A_{10}}{10^{-7} \text{ s}^{-1}} \right)^{-1} Q_{10}^{-1} \frac{S_{[\text{CI}]}}{[\text{Jy km s}^{-1}]} [M_{\odot}], \quad (2)$$

where X_{CI} is the [CI]-to-H₂ abundance ratio (we assume $X_{\text{CI}} = 3 \times 10^{-5}$), A_{10} is the Einstein A-coefficient ($A_{10} = 7.93 \times 10^{-8} \text{ s}^{-1}$), and Q_{10} is the excitation factor which depends on the kinetic temperature, and density of the gas (we adopt $Q_{10} = 0.5$). The cosmology dependence is included through the luminosity distance, D_l . Using the observed integrated intensity of the [CI] $^3P_1-^3P_0$ line in APM 08279+5255 gives $M_{\text{H}_2-[\text{CI}]} = (2.7 \pm 0.4)m^{-1} \times 10^{11} M_{\odot}$, in good agreement with the molecular gas mass estimated from the CO J=1-0 line.

Table 2 presents the molecular gas mass estimates derived from [CI] and from CO for the five high-redshift objects where both lines are detected, adjusted to a common cosmology. The [CI] $^3P_1-^3P_0$ line integrated intensities for IRAS F10214, SMM J14011+0252, and

H1413+117 are taken from Weiss et al. (2005), and for PSS 2322+1944 from Pety et al. (2005). The CO J=1-0 line has been detected only in APM 08279+5255 and PSS 2322+1944 (Carilli et al. 2002). For the other objects, which are not detected in the CO J=1-0 line, we use observations of the CO J=3-2 line (IRAS F10214; Solomon et al. 1992, H1413+117; Weiss et al. 2003, SMM J14011+0252; Downes & Solomon 2003), which is approximately equal to the luminosity in the CO J=1-0 line at high-redshifts for warm, dense gas (Solomon et al. 1992). Though the uncertainties are large, there is very good agreement between the molecular gas mass estimates from the two tracers.

4.4. H₂O

We did not detect any significant H₂O 1₁₀–1₀₁ line emission in APM 08279+5255. We can estimate the H₂O line luminosity expected for the circumnuclear region for a nominal water abundance, again adopting the previously derived physical conditions for the region. In Galactic molecular clouds, a typical ortho-H₂O abundance is 4.5×10^{-9} relative to H₂ (Snell et al. 2000; Ashby et al. 2000). For $T_{kin} = 80$ K, $n_{H_2} \sim 40,000$ cm⁻³, an LVG calculation gives $N(\text{H}_2\text{O})/\Delta v = 8.0 \times 10^{12}$ cm⁻²(km s⁻¹)⁻¹, $L'_{\text{H}_2\text{O}} = 1.1 \times 10^7$ K km s⁻¹ pc², more than two orders of magnitude below the upper limit. In strongly shocked regions, the H₂O abundance has been observed to be enhanced by more than an order of magnitude, but even if that were the case, calculations show that the H₂O 1₁₀–1₀₁ line emission would remain well below the achieved detection threshold.

5. Summary

We detected [CI] ³P₁–³P₀ line emission in the ultraluminous quasar APM 08279+5255 at $z=3.91$. The [CI] ³P₁–³P₀ line width and center are similar to those of previously detected millimeter CO and HCN lines. Estimates of the molecular gas mass based on the [CI] ³P₁–³P₀ line and based on CO lines yield similar results, and there is no evidence for any substantial contribution from a primarily atomic medium. Though the observational uncertainties remain large, this seems to be the case for the five high-redshift sources with reported detections of both CO and [CI] emission lines. The [CI] ³P₁–³P₀ line may be a valuable alternative probe of molecular gas mass in systems lacking high excitation CO line emission, where the molecular medium is more diffuse and cooler ($T_{kin} \lesssim 20$ K, and $n_{H_2} \lesssim 10^4$ cm⁻³; Papadopoulos et al. 2004a). The Atacama Large Millimeter Array will greatly expand the number of high-redshift sources accessible in [CI] and CO emission, and will have the capability to spatially resolve the emission to show directly the extent of the

gas.

6. Acknowledgments

We thank the IRAM PdBI staff for carrying out these observations. J.W. is grateful to the SAO for support through a predoctoral student fellowship and the Department of Astrophysics at INAOE for a graduate student scholarship. This work is partially supported by CONACYT grant 39953-F. J.W. thanks Sébastien Muller for helpful tips on PdBI data reduction, and also Padelis Papadopoulos and Matthew Ashby for discussions about [CI] and H₂O excitation and emission at high-redshift. We thank the referee for a thorough reading of the submitted manuscript and helpful suggestions.

REFERENCES

- Ashby, M. L. N., et al. 2000, *ApJ*, 539, L115
- Barvainis, R., Maloney, P., Antonucci, R., Alloin, D., 1997, *ApJ*, 484, 695
- Carilli C. L., Cox P., Bertoldi F., Menten K. M., Omont A., Djorgovski S. G., Petric A., Beelen A., Isaak K. G., McMahon R. G. 2002, *ApJ*, 575, 145
- Casoli F., Gerin M., Encrenaz P. J., Combes F., 1994, *A&A*, 287, 716
- Combes, F. & Wiklind, T. 1997, *ApJ* 486, L79
- Downes, D. & Solomon, P.M. 1998, *ApJ*, 507, 615
- Downes D., Neri R., Wiklind T., Wilner D. J., Shaver P. A. 1999, *ApJ*, 513, L1 (D99)
- Downes, D. & Solomon, P.M. 2003, *ApJ*, 528, 37
- Egami E., Neugebauer G., Soifer B. T., Matthews K., Ressler M., Becklin E. E., Murphy T. W., Dale D. A., 2000, *ApJ*, 535, 561
- Ellison S. L., Lewis G. F., Pettini M., Sargent W. L. W., Chaffee F. H., Foltz C. B., Rauch M., Irwin M. J., 1999, *PASP*, 111, 946
- Encrenaz P. J., Combes F., Casoli F., Gerin M., Pagani L., Horellou C., Gac C., 1993, *A&A*, 273, L19
- Gallagher S. C., Brandt W. N., Chartas G., Garmire G. P., 2002, *ApJ*, 567, 37
- Garcia-Burillo S., et al., 2006, *astro-ph/0605656*
- Gérin M. & Phillips T.G. 1998, *ApJ*, 509, L17

- Gérin M. & Phillips, T.G. 2000, ApJ, 537, 644
- Ibata R. A., Lewis G. F., Irwin M. J., Lehár J., Totten E. J., 1999, AJ, 118, 1922
- Irwin M. J., Ibata R. A., Lewis G. F., Totten E. J., 1998, ApJ, 505, 529
- Lewis, G.F., Chapman, S.C., Ibata, R.A., Irwin, M.J., & Totten, E.J. 1998, ApJ, 505, L1
- Lewis, G.F., Carilli, C., Papadopoulos, P., Ivison, R.J., 2002, MNRAS, 330, L15
- Maloney, P.R., Hollenbach, D.J., Tielens, G.G.M. 1996, ApJ, 466, 561
- Papadopoulos, P., Ivison, R.J., Carilli, C., Lewis, G. 2001, Nature, 409, 58
- Papadopoulos, P.P., Thi, W.-F., Viti, S. 2004a, MNRAS, 351, 147
- Papadopoulos, P.P. & Greve, T.R. 2004b, ApJ, 615, L29
- Papadopoulos P. P., 2005, ApJ, 623, 763
- Pety J., Beelen A., Cox P., Downes D., Omont A., Bertoldi F., Carilli C. L. 2005, A&A, 428, L21
- Sanders, D.B., Soifer, B.T., Elias, J.H., Madore, B.F., Matthews, K., Neugebauer, G., & Scoville, N.Z. 1988, ApJ, 325, 74
- Sanders, D.B. & Mirabel, I.F. 1996, ARA&A, 34, 749
- Schilke, P., Carlstrom, J.E., Keene, J., Phillips, T.G., 1993, ApJ, 417, L67
- Schöier, F.L., van der Tak, F.F.S., van Dishoek, E.F., Black, J.H., 2005, A&A, 432, 369
- Snell, R. L., et al. 2000, ApJ, 539, L101
- Soifer B. T., et al. 2004, ApJS, 154, 151
- Solomon, P.M., Downes, D., Radford, S.J.E., 1992, ApJ, 398, L29
- Spergel D. N., et al., 2006, astro-ph/0603449
- Wagg J., Wilner D. J., Neri R., Downes D., Wiklind T. 2005, ApJ, 634, L13
- Weiss A., Henkel C., Downes, D., Walter F. 2003, A&A, 409, L41
- Weiss A., Downes D., Henkel C., Walter F. 2005, A&A, 429, L25
- White, G.J., Ellison, B., Claude, S., Dent, W.R.F., Matheson, D.N., 1994, A&A, 284, L23

Table 1. [CI] $^3\text{P}_1-^3\text{P}_0$ line parameters for APM 08279+5255.

[CI] $^3\text{P}_1-^3\text{P}_0$ peak:	2.20 ± 0.51 mJy
[CI] $^3\text{P}_1-^3\text{P}_0$ ΔV_{FWHM} :	386 ± 67 km s $^{-1}$
[CI] $^3\text{P}_1-^3\text{P}_0$ v_0^{a} :	117 ± 28 km s $^{-1}$
$S_{[\text{CI}]}$:	0.93 ± 0.13 Jy km s $^{-1}$
$L'_{[\text{CI}]}^{\text{b}}$:	$3.1 \pm 0.4 \times 10^{10}$ K km s $^{-1}$ pc 2

^avelocity with respect to $z=3.911$, determined from CO lines.

^bThe [CI] $^3\text{P}_1-^3\text{P}_0$ luminosity is not corrected for lensing magnification.

Table 2. Masses of neutral carbon and H₂ in high-redshift objects.

Object	z_{CO}^a	$M_{[CI]}$ [M _⊙ /10 ⁷]	$M_{H_2}(CO)$ [M _⊙ /10 ¹⁰]	$M_{H_2}([CI])$ [M _⊙ /10 ¹⁰]	Refs. CO,[CI]
IRAS F10214	2.29	$(2.7 \pm 0.3)m^{-1}$	$(11.3 \pm 2.5)m^{-1}$	$(18.8 \pm 2.4)m^{-1}$	1,2
H1413+117	2.56	$(8.1 \pm 1.2)m^{-1}$	$(44.3 \pm 0.7)m^{-1}$	$(55.8 \pm 8.6)m^{-1}$	3,2
SMM J14011+0252	2.57	$(3.7 \pm 0.6)m^{-1}$	$(9.5 \pm 1.0)m^{-1}$	$(25.9 \pm 4.3)m^{-1}$	4,2
APM 08279+5255	3.91	$(4.4 \pm 0.6)m^{-1}$	$(13.4 \pm 3.0)m^{-1}$	$(26.7 \pm 3.7)m^{-1}$	5,6
PSS 2322+1944	4.12	$(3.8 \pm 0.6)m^{-1}$	$(12.5 \pm 5.3)m^{-1}$	$(25.2 \pm 3.7)m^{-1}$	7,8

^aRedshift of CO emission.

Note. — m is the gravitational lensing magnification factor

References – (1) Solomon et al. 1992; (2) Weiss et al. 2005; (3) Weiss et al. 2003; (4) Downes & Solomon 2003; (5) Lewis et al. 2002; (6) This paper; (7) Carilli et al. 2002; (8) Pety et al. 2005

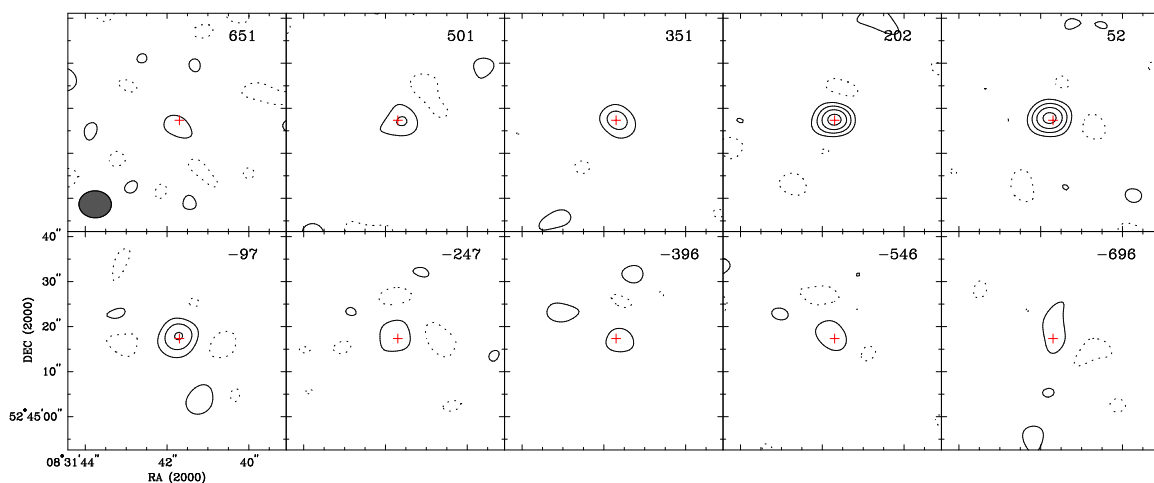


Fig. 1.— Images of the $[\text{CI}] \ ^3\text{P}_1\text{--}^3\text{P}_0$ and 100.2 GHz continuum emission in APM 08279+5255 over the full observed velocity range. The contour intervals are -2, 2, 4, 6 and $8 \times \sigma$ ($0.36 \text{ mJy beam}^{-1}$). The cross marks the position of the CO peak position from D99, which is offset ($1''.19, -0''.36$) from the phase center ($08^{\text{h}}31^{\text{m}}41^{\text{s}}.57, 52^{\circ}45^{\text{m}}17^{\text{s}}.7$). The filled ellipse in the top left panel shows the $7''.2 \times 6''.0$ PA 89.0° synthesized beam. The velocities indicated in the upper right corner in each panel are relative to $z=3.911$, determined from CO observations. .

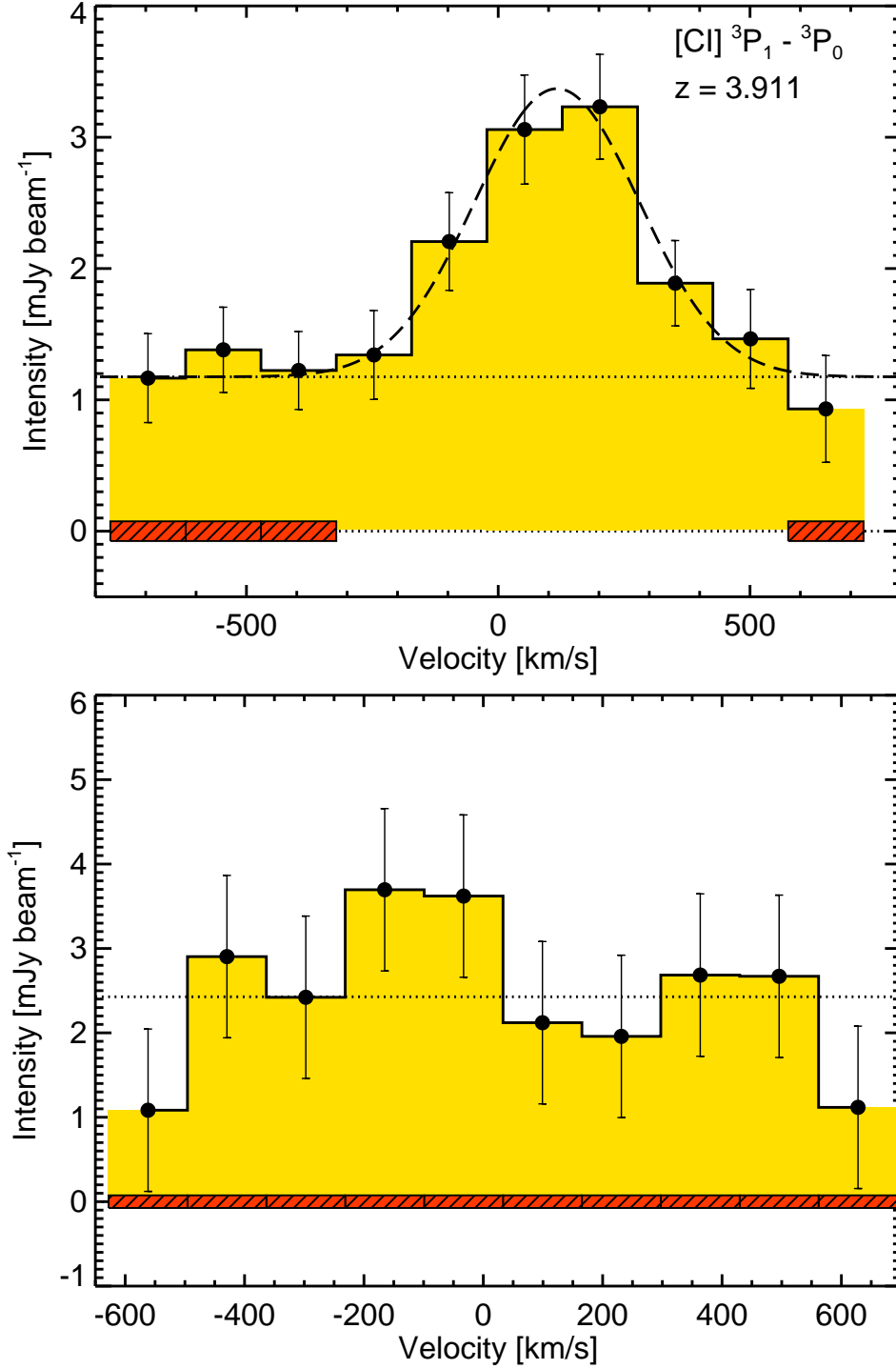


Fig. 2.— Spectra of [CI] $^3P_1 - ^3P_0$ (*top*) and H $_2$ O $1_{10} - 1_{01}$ (*bottom*) at the position of peak continuum intensity. Dotted lines show the fitted continuum levels, calculated from the intensity in the channels marked by the hatched regions. The dashed line shows a Gaussian fit to the [CI] $^3P_1 - ^3P_0$ emission.